High-pressure studies on YNi_2B_2C at room temperature

S. Meenakshi, V. Vijayakumar, R. S. Rao, B. K. Godwal, and S. K. Sikka
High Pressure Physics Division, Bhabha Atomic Research Centre, Mumbai 400085, India

P. Ravindran
Condensed Matter Theory Group, Department of Physics, Uppsala University, Box 530, 75121 Uppsala, Sweden

Z. Hossain, R. Nagarajan, and L. C. Gupta
Tata Institute of Fundamental Research, Colaba, Mumbai 400005, India

R. Vijayaraghavan
SAMEER, I.I.T. Campus, Mumbai 400076, India

(Received 29 April 1997; revised manuscript received 16 March 1998)

The electronic and lattice structure, and equation of state behavior of YNi_2B_2C has been investigated by electrical resistivity, thermoelectric power, and angle-dispersive x-ray-diffraction measurements. The electrical resistance under pressure has also been measured for other lanthanide-nickel borocarbides (RNi_2B_2C, R=Ho, Er, and Tm). The high pressure behavior is analyzed by electronic band-structure [tight-binding linear muffin-tin orbital (LMTO) and full-potential LMTO] calculations on YNi_2B_2C. The measured thermoelectric power shows a peak around 2 GPa pressure. X-ray powder diffraction measurements of the lattice parameter under pressure reveal that the carbon-filled variant of $ThCr_2Si_2$-type tetragonal structure prevailing under ambient conditions is preserved in YNi_2B_2C up to 6 GPa. Pressure-volume data on YNi_2B_2C yielded a bulk modulus of 200 GPa. This is in agreement with the value computed by the first-principles electronic-structure calculations. It is also shown that the observed peak in the thermoelectric power in YNi_2B_2C and the weak pressure dependence of the superconducting-transition temperature can be correlated with the details of the electronic density of states. [S0163-1829(98)04430-0]

I. INTRODUCTION

The family of lanthanide nickel borocarbide (RNi_2B_2C where R=lanthanide) superconductors have attracted much attention during the last few years.[1–4] Their crystal structure is a carbon-filled variant of the $ThCr_2Si_2$-type tetragonal body-centered (space group $I4/mmm$) structure.[5] The nickel boride framework of the structure is modified by the insertion of carbon in the lanthanide layer, directly between the boron atoms, thus forming a cage of the lanthanide. The addition of carbon in the lanthanide plane manifests itself in the expansion of the *c*-axis lattice parameter and the contraction of the *a*-axis lattice parameter. These structural modifications lead to some interesting features, such as (i) short B-C separation of 1.46 Å; (ii) near ideal tetrahedral coordination of Ni atoms with four neighboring B atoms; and (iii) Ni-Ni separation of 2.45 Å, which is shorter than in Ni metal, indicating that the Ni-Ni bonds might be very strong. The superconducting transition temperature, T_c, of these materials shows interesting high-pressure behavior.[6,7] For example, in Ho and Tm borocarbides, T_c decreases with pressure (dT_c/dP at ambient pressure is -0.25 K/GPa for $HoNi_2B_2C$, and -0.45 K/GPa for $TmNi_2B_2C$), whereas in $ErNi_2B_2C$ T_c increases with pressure ($dT_c/dP=+0.17$ K/GPa).[7] But in YNi_2B_2C there is only a weak variation of T_c ($dT_c/dP=+0.03$ K/GPa at normal pressure) with pressure. The larger pressure dependence of T_c in Ho and Tm based borocarbides has been attributed to magnetic correlation.[7] It is well known that the pressure affects T_c via changes in the phonon density of states and electron density of states at the Fermi level (E_F).[8] Also, the changes in the electronic and phonon spectra might lead to structural transitions and affect the transport properties like electrical resistance and thermoelectric power (TEP). Hence, we have carried out the angle-dispersive x-ray-diffraction (ADXRD) measurements at room temperature and high pressures on YNi_2B_2C to obtain the equation of state and to look for any signature of structural transition in it. Electrical resistance and TEP measurements have also been performed. We have carried out electronic-structure calculations (at 0 K) at high pressures, which include the experimentally applied pressure conditions to interpret the experimental data. Band-structure calculations for ambient pressure have been reported earlier on $LuNi_2B_2C$ (Refs. 9 and 10) and YNi_2B_2C.[11]

II. EXPERIMENTAL DETAILS

For electrical resistivity and TEP measurements, pellets of the samples of approximate size, 3×5 mm with a thickness of 0.2 mm, were taken, and then pressed between tungsten carbide anvils to a load of 5 tons. The well-compacted material was then trimmed to pieces of 1.5 mm long and 2.5 mm wide. An opposed Bridgeman anvil setup,[12] consisting of 12 mm face diameter tungsten carbide anvil pairs, was used. Resistance was measured by the four-probe technique. Pressure calibration was done *in situ* by using Bi. The samples, along with a talc pressure medium, were encapsulated in two 0.15-mm thick pyrophylite gaskets. Thin mylar

sheets protected the sample from direct contact with talc and also ensured good electrical contact by preventing talc from entering the sample and electrical leads. For TEP measurements,[13] chromel-alumel thermocouple wires of 0.25 mm ϕ were employed. No corrections for the variation of the thermo-emf of chromel alumel were applied, as they are negligible. Thermocouple wires were held in position within the gaskets by grooves on it and over the sample by a thin mylar sheet taped to the anvil. The ADXRD measurements employed a photostimulable fluorescent plate (commonly known as an imaging plate) as an area detector.[14] Resistivity measurements under pressure were carried out on YNi_2B_2C, $HoNi_2B_2C$, $ErNi_2B_2C$, and $TmNi_2B_2C$. High-pressure x ray diffraction and TEP measurements were made only on the YNi_2B_2C samples. For ADXRD measurements, a YNi_2B_2C powder sample of 5μ size, along with a ruby pressure marker, was loaded in a Bassett-type diamond-anvil cell in which an ethanol-methanol mixture was used as a pressure transmitter.

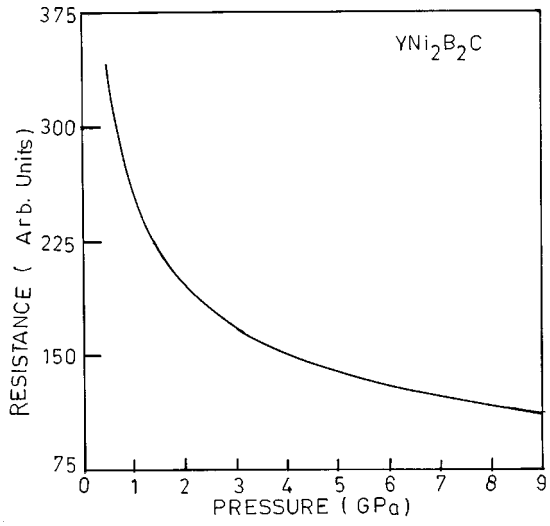

FIG. 1. Variation of the electrical resistance with pressure for YNi_2B_2C.

III. THEORETICAL CALCULATIONS

We have carried out the first-principles total-energy calculations by the tight-binding linear muffin-tin orbital (TB-LMTO) method[15] within the framework of the atomic sphere approximation (ASA). Within this approximation, the atom and orbital decomposition of the electron density of states is well defined. This decomposition will be used below (Sec. IV) in interpreting some experimental observations. The self-consistent band-structure calculations were done on YNi_2B_2C using the scalar relativistic version of TB-LMTO with the frozen core approximation. The atomic levels $4d^15s^2$ of Y, $3d^94s^1$ of Ni, $2s^22p^1$ of B, and $2s^22p^2$ of C were treated as valence electron states. Lattice constants and atomic positions in the unit cell were obtained from Ref. 16. The ratios of atomic sphere radii were optimized so that the theoretically estimated equilibrium volume would agree with the experimental data. We obtained the ratios as Y : Ni : B : C = 1.0 : 0.79 : 0.52 : 0.5, which are in agreement with an earlier work.[17] The Barth-Hedin exchange[18] was used throughout. The eigenvalue problem was solved by considering the *s*, *p*, and *d* partial waves only without downfolding any of the orbitals. Apart from this, the combined correction terms, which account for the nonspherical shape of the atomic cells and the truncation of higher partial waves ($l>2$) inside the spheres, were also included to improve the accuracy of the LMTO method. The tetrahedron method for the Brillouin-zone integrations (**k**-space integrations) was used. The eigenvalues were obtained with a set of 349 **k** points in the irreducible wedge of the first Brillouin zone (BZ) of the body-centered tetragonal lattice of YNi_2B_2C. The total energies at various volume fractions were fitted to a polynomial to calculate the pressure.

In order to improve upon the accuracy in the total energy and equation of state, we carried out the calculations by the full-potential LMTO (FP-LMTO) method. The all electron FP-LMTO calculations employed no shape approximation to the charge density or potential.[19] The spherical harmonic expansion of the charge density, potential, and basis functions were carried out up to $l_{max}=8$. Thus, the basis set comprised augmented linear muffin-tin orbitals containing 4*s*, 4*p*, 5*s*, 5*p*, 4*d*, 4*f* of Y; 3*p*, 3*d*, 4*s*, 4*p* of Ni; 2*s*, 2*p*, and 3*d* of B and C. Further, two sets of energy parameters, one with energies appropriate to the semicore bands and the other with energies corresponding to the valence bands, were used to calculate the radial functions in the muffin-tin spheres. Also, two tail energies were used for every state. Approximate orthogonality between bases with the same *l* value was maintained by energy separation. Integration over the BZ was done using ''special point sampling.''[20] The results reported here used 75 **k** points in the irreducible wedge of the BZ. The self-consistent iterations were continued until the total-energy differences between two consecutive iterations were less than 10^{-6} Ry. The equation of state obtained with FP-LMTO calculations show better agreement with our ADXRD estimates at higher compressions. However, the calculated equilibrium volume by FP-LMTO departed more from the experimental value (see discussion in Sec. IV below). It was felt that the nonlocal corrections to the local-density approximation, as adopted in the generalized gradient approximation (GGA) for the exchange correlation terms, may be important here.[21] Hence, we carried out additional FP-LMTO calculations with GGA. The gradient terms were evaluated in these calculations for the full nonspherical charge density in the muffin-tin spheres as well as in the interstitial region.[19]

The atom and orbital decomposition of the electron density of states (DOS) was carried out by the LMTO-ASA method. In view of the anisotropic nature of the structure, the value of the ratio *c/a* of the lattice parameters *c* and *a* at various compressions was optimized by the FP-LMTO total-energy calculations. These accurate full-potential calculations are necessary as the changes involved are small. The *c/a* value that gives the minimum total energy at the chosen compression was then used in the LMTO-ASA calculations to get the atomic and orbital components of the DOS.

IV. RESULTS AND DISCUSSION

In all cases, YNi_2B_2C, $HoNi_2B_2C$, $ErNi_2B_2C$, and $TmNi_2B_2C$, electrical resistance showed a smooth variation with pressure with no discontinuity up to about 8 GPa. Fig-

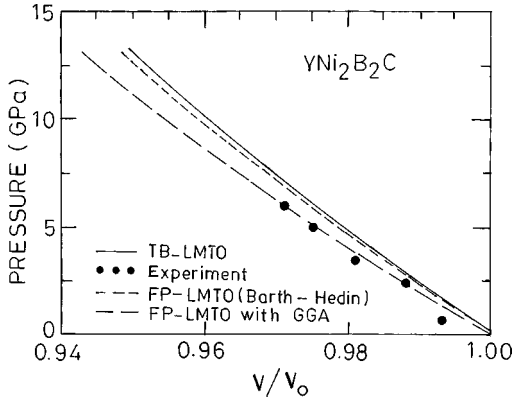

FIG. 2. Equation of state for YNi_2B_2C.

ure 1 shows the typical data for YNi_2B_2C. This kind of smooth variation indicates the absence of a structural phase transition and is consistent with ADXRD measurements discussed below. The initial sharp fall up to 2 GPa is in contrast to the resistance versus pressure behavior seen usually in metals like Ag and Au.

The ADXRD measurements on YNi_2B_2C showed that the structure prevailing at ambient conditions, i.e., a variant of

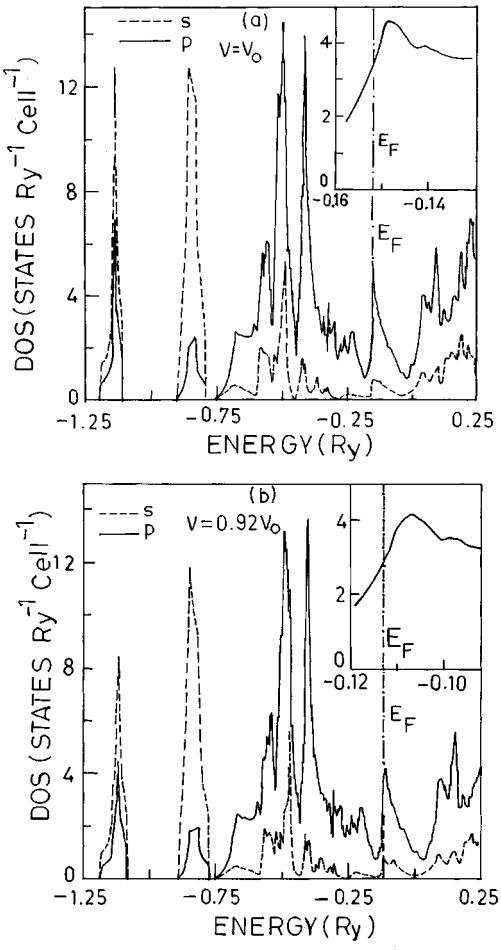

FIG. 3. Boron *s*- and *p*-component density of states (per primitive cell) in YNi_2B_2C at (a) normal volume, and (b) relative volume ratio $V/V_0=0.92$ (corresponding to a pressure of about 22 GPa). The insets at the top right-hand corners show the boron *p*-component peak near the Fermi level in an expanded scale.

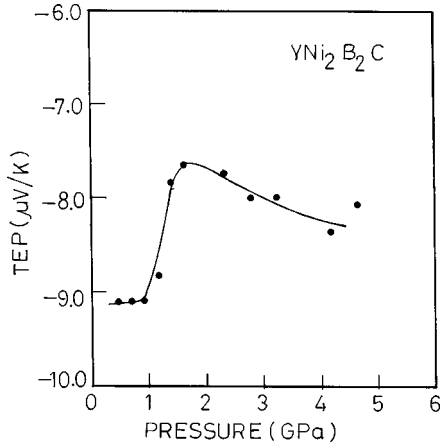

FIG. 4. Thermoelectric power as a function of pressure for YNi_2B_2C.

the layered $ThCr_2Si_2$-type tetragonal structure with carbon atoms in the *Y* plane,[5] is retained up to 6 GPa. The equation of state obtained from the measured lattice parameters is shown in Fig. 2. This yields a bulk modulus of 200 GPa, which is large compared to the value for most of the metals (which is in the range of 50 to 100 GPa).

The equilibrium volume calculated by the TB-LMTO method is less by 1.5% of the experimental value, which is typical of the local-density approximation based calculations. The theoretical equation of state compares well with the measured $(P\text{-}V)$data for initial compressions, and yields a bulk modulus of about 210 GPa.[22,23] However, the theoretical equation of state is stiffer at higher compressions (Fig. 2). The FP-LMTO calculations yield the equation of state curve that is slightly in better agreement with our ADXRD measurements. The equilibrium volume, however, is underestimated by about 6%. Further, the application of GGA in the FP-LMTO calculations lowers this deviation from the experimental value from 6% to 2% and gives excellent agreement with our ADXRD data. The FP-LMTO calculations with GGA yield the bulk modulus of 190 GPa.

The calculated *c/a* ratio at various compressions agree within 1% of the estimates from our ADXRD experiments. For example, at $V/V_0=0.97$, the theoretical estimate gives $c/a = 2.931$ as compared to our ADXRD value of 2.948. Both the FP-LMTO calculations and the ADXRD data show less than a 1% increase in the *c/a* ratio for the 3% compression in volume (i.e., an increase in pressure by about 6 GPa).

It has been shown that, in this class of materials, T_c is influenced by the boron component of the electron DOS at E_F.[10] This is because these states couple strongly to the phonons involving boron displacements in NiB_4 tetrahedra.[10] Our calculations (TB-LMTO) give the DOS at ambient pressure in reasonable agreement with those available in the literature for YNi_2B_2C.[11,24] They also show that the boron component of the DOS is reduced at E_F on compression. Apart from the usual band broadening effect, the DOS peak that is just above E_F moves slowly away from it to higher energies under compression [compare Figs. 3(a) and 3(b)]. In the pressure range up to 2 GPa (where T_c data are available[6,7]), the change in the boron component DOS at E_F as obtained by the present calculations is so small that almost

no change in T_c is expected. This is consistent with the experimental findings.[6,7]

Our TEP result, shown in Fig. 4, exhibits a peak around 2 GPa pressure.[25] As is well known, the diffusion based thermopower depends on the energy derivative of the DOS at E_F, and is dominated by the *d* component.[26] Our calculations show a sharp Ni *d*-component peak in the vicinity of E_F (not shown). This peak also shifts slowly away from E_F to higher energies under compression, as does the boron *p*-component peak shown in Fig. 3. Thus, we conjecture that the observed broad peak in the pressure dependence of TEP is due to a slow shift of the Ni *d*-based bands with respect to E_F to higher energies which leads to changes in the Fermi-surface topology.[27]

In summary, we have performed high-pressure investigations at room temperature for the borocarbide superconductor YNi_2B_2C, by electrical resistivity, thermoelectric power, and angle-dispersive x-ray-diffraction techniques. The electrical resistivity up to 8 GPa does not indicate any structural transition. This is confirmed by ADXRD measurements up to the pressure of 6 GPa. FP-LMTO calculations with GGA give the best agreement with the pressure-volume data from ADXRD measurements which yield a bulk modulus of 200 GPa. The observed broad peak in the TEP measurements may be related to the shift of the Ni *d*- based bands with respect to E_F to higher energies. The weak dependency on pressure of T_c in YNi_2B_2C is consistent with insignificant changes, due to compression, in the calculated DOS at E_F of the boron component peak.

ACKNOWLEDGMENT

One of us (P.R.) wishes to acknowledge Börje Johansson, Olle Eriksson, and J. M. Wills for their encouragement.

[1] Chandan Mazumdar, R. Nagarajan, C. Godart, L. C. Gupta, M. Latroche, S. K. Dhar, C. Levy-Clement, B. D. Padalia, and R. Vijayaraghavan, Solid State Commun. **87**, 413 (1993).

[2] R. Nagarajan, Chandan Mazumdar, Z. Hossain, S. K. Dhar, K. V. Gopalakrishnan, L. C. Gupta, C. Godart, B. D. Padalia, and R. Vijayaraghavan, Phys. Rev. Lett. **72**, 274 (1994).

[3] R. J. Cava, H. Takagi, H. W. Zandbergen, J. J. Krajewski, W. F. Peck, T. Siegrist, B. Batlogg, R. B. Van Dover, R. J. Felder, K. Mizuhashi, J. O. Lee, H. Elsaki, and S. Uchida, Nature (London) **367**, 252 (1994).

[4] See, for example, J. Low Temp. Phys. **105**, issues 3/4, 5/6 (1996); **107**, issue 5/6 (1997); Czech J. Phys. **46**, suppl. (1996); Physica B **230-232** (1997).

[5] T. Siegrist, H. W. Zandbergen, R. J. Cava, J. J. Krajewski, and W. F. Peck, Nature (London) **367**, 254 (1994).

[6] H. Schmidt and H. F. Braun, Physica C **229**, 315 (1994).

[7] E. Alleno, J. J. Neumeier, J. D. Thompson, P. C. Canfield, and B. K. Cho, Physica C **242**, 169 (1995).

[8] P. B. Allen and R. C. Dynes, Phys. Rev. B **12**, 905 (1975).

[9] W. E. Pickett and D. J. Singh, Phys. Rev. Lett. **72**, 3702 (1994).

[10] L. F. Mattheiss, T. Siegrist, and R. J. Cava, Solid State Commun. **91**, 587 (1994)

[11] D. J. Singh, Solid State Commun. **98**, 899 (1996); J. I. Lee, T. S. Zhao, I. G. Kim, B. I. Min, and S. J. Youn, Phys. Rev. B **50**, 4030 (1994).

[12] V. Vijayakumar, B. K. Godwal, Y. K. Vohra, S. K. Sikka, and R. Chidambaram, J. Phys. F **14**, L65 (1984).

[13] A. K. Singh and Geetha Ramani, Rev. Sci. Instrum. **49**, 1324 (1978); Viswanathan Vijayakumar, Sudhir N. Vaidya, Echur V. Sampathkumaran, and Laxmi C. Gupta, High Temp.-High Press. **12**, 649 (1980).

[14] See Ref. 23 for details; the IP system is based on a 425E Molecular Dynamics phosphor imager model; O. Shimomura and K. Takemura, Rev. Sci. Instrum. **63**, 967 (1992).

[15] O. K. Andersen and O. Jepsen, Phys. Rev. Lett. **53**, 2571 (1984).

[16] B. C. Chakoumakos, C. Chakoumakos and M. Paranthaman, Physica C **227**, 143 (1994).

[17] P. Ravindran, S. Sankaralingam, and R. Asokamani, Phys. Rev. B **52**, 12 921 (1995).

[18] U. Von Barth and L. Hedin, J. Phys. C **5**, 1629 (1972).

[19] J. M. Wills and B. R. Cooper, Phys. Rev. B **36**, 3809 (1987); D. L. Price and B. R. Cooper *ibid.* **39**, 4945 (1989).

[20] D. J. Chadi and M. L. Cohen, Phys. Rev. B **8**, 5747 (1973); S. Froyen, Phys. Rev. B **39**, 3168 (1989).

[21] J. P. Perdew, J. A. Chevary, S. H. Vosko, K. A. Jackson, M. R. Pederson, D. J. Singh, and C. Fiolhais, Phys. Rev. B **46**, 6671 (1992).

[22] We had earlier obtained (Ref. 23) the bulk modulus as 270 GPa, taking the atomic radii ratios of Y : Ni : B : C in YNi_2B_2C, the same as Lu : Ni : B : C in $LuNi_2B_2C$ [= 1.0 : 0.833 : 0.5 : 0.474 (Ref. 9)].

[23] S. Meenakshi, V. Vijayakumar, R. S. Rao, B. K. Godwal, S. K. Sikka, Z. Hossain, R. Nagarajan, L. C. Gupta, and R. Vijayaraghavan, Physica B **223&224**, 93 (1996).

[24] We get the DOS at E_F of 3.8 states/eV per primitive cell as compared to the values of 4.3 and 4.0 in Refs. 11, respectively. The peak near E_F in our calculations lies 40 meV above the Fermi level, whereas the linear augmented plane-wave calculations of Singh (Ref. 11) show the peak 25 meV above E_F.

[25] The preliminary data of TEP were presented in Ref. 23. The oscillations reported there (plotted as $S_{ambient}$-$S_{underpressure}$) were not observed in the repeated measurements. The data shown in the present paper are based on two independent runs.

[26] F. J. Blatt, P. A. Schroeder, C. L. Foiles, and D. Greig, *Thermoelectric Power of Metals* (Plenum, New York, 1976).

[27] L. M. Lifshitz, Zh. Eksp. Teor. Fiz. **38**, 1569 (1960) [Sov. Phys. JETP **11**, 1130 (1960)]; L. Dagens, J. Phys. (France) Lett. **37**, 137 (1976); J. Phys. F **8**, 2093 (1978).